

1 **Chromatic contrast in luminance-defined images affects performance and neural activity during a**
2 **shape classification task**

3

4 Ben J Jennings^{1,2}

5 Jasna Martinovic¹

6 1 - School of Psychology, University of Aberdeen, UK

7 2- McGill Vision Research, Department of Ophthalmology, McGill University, Montreal, Canada

8

9 Pages: 26 (including Figures in line with text)

10 Figures: 10

11 Tables: 0

12 Supplementary materials: 2

13

14 Corresponding author: Dr Jasna Martinovic, School of Psychology, University of Aberdeen, William
15 Guild Building, Aberdeen, AB24 3UB, UK

16 email: j.martinovic@abdn.ac.uk

17 phone: +44 1224 272 240

18

19 Running title: Effects of chromatic contrast in shape classification

20

21

22

1 **Abstract**

2 Models of object recognition generally emphasise the importance of luminance-defined shape.
3 However, it is still not fully understood how colour signals combine with luminance signals to affect
4 object-related form processing. This electroencephalographic study aimed to examine the
5 contribution of chromatic contrast by assessing its effects on the time-course of shape-related
6 processing. Participants classified Gaborised images of object shapes, non-object shapes and patches
7 of pseudo-randomly scattered Gabors. Stimuli excited either the luminance (L+M) channel alone,
8 luminance and L-M channels, or luminance, L-M and S-(L+M) channels and were presented either at
9 mean discrimination threshold or at twice this mean threshold. As expected, classification accuracy
10 was comparable at threshold, as were the attributes of the early, perceptual N1 component of the
11 event-related potential (ERP). Differences emerged at suprathreshold: objects defined by the full
12 combination of channels were associated with the poorest performance and the lowest N1
13 amplitude. Shape-sensitivity was not consistently observed in the N1 but was more evident in the
14 late positive potential (LPP), a cognitive ERP component. Both the N1 and the LPP were affected by
15 the amount and type of contrast in the image. Whilst the effects of luminance and L-M contrast
16 were similar, affecting the ERP selectively during the N1 and LPP period, S-(L+M) contrast elicited a
17 sustained shift in amplitude. Our results demonstrate, for the first time using a combination of
18 behavioural as well as early and late electrophysiological effects, that shape classification is
19 determined by both the chromatic and the luminance content of the image.

20

21 Keywords: object representation, shape perception, luminance, chromatic mechanisms, contrast,
22 EEG.

23

1 Introduction

2 Acquiring knowledge about objects is essential for adaptive behaviour in everyday
3 environments. Both achromatic and chromatic information are relevant for everyday vision but their
4 contributions to object processing have traditionally been perceived as different, with luminance
5 seen as more relevant for shape processing and colour seen as more relevant for segmenting objects
6 from their backgrounds (Tanaka, Weiskopf, & Williams, 2001). This is reflected in models of object
7 recognition. For example, low-level inputs that drive object processing in Sowden and Schyns' (2006)
8 model stem from luminance-driven spatial frequency channels. Further, in Bar's model of object
9 recognition, the fast, top-down input essential for constraining the processing in posterior
10 representational areas is driven by rapid projections of low-spatial frequency luminance information
11 (Bar, 2003). At the neuronal level, the tuning of luminance-driven spatial frequency channels is
12 affected by lateral inhibition between neurons with spatially overlapping receptive fields which are
13 tuned to different spatial frequency and orientation bands (Greenlee & Magnussen, 1988; Tolhurst,
14 1972). Lateral interactions also exist between spatial frequency channels sensitive to different
15 spatial locations: Polat and Sagi (1993) found that foveal target detection is affected by a narrow
16 inhibitory surround and a further much larger facilitatory area. In this way, neuronal sensitivity is
17 fine-tuned to spatial variations of luminance contrast that define shape across orientation and size.

18 However, there is emerging evidence that colour signals can and do contribute to the
19 processing of object form. To a degree, colour mechanisms are also able to provide low-level
20 information that sustains object recognition, with spatial frequency (Mullen & Losada, 1994; Mullen
21 & Losada, 1999) and orientation (Webster, DeValois, & Switkes, 1990; Wuerger, Morgan, Westland,
22 & Owens, 2000) channels that are not vastly dissimilar to those driven by luminance information.
23 Anatomical and physiological investigations found that a substantial amount of neurons in areas V1
24 and V2 of the cortex receives inputs from different visual streams, indicating that the segregation of
25 luminance and colour signals is not as normative as had been previously thought (Levitt, Yoshioka, &
26 Lund, 1994; Vidyasagar, Kulikowski, Lipnicki, & Dreher, 2002; for models, see Lund, Wu, Hadingham,
27 & Levitt, 1995, Zhaoping, 2014; for comprehensive reviews see Kulikowski, 2003; Solomon & Lennie,
28 2007). Benefits brought about by the availability of spatial information from both luminance and
29 colour might be expected from considerations of the complexities of our everyday visual
30 environments. Contributions of chromatic signals to form processing might be particularly salient
31 due to their independence from shadows and shading, which are defined through changes in
32 luminance only (for a review, see Shevell & Kingdom, 2008). Indeed, edge extraction from luminance
33 and chromatic spatially superimposed components within a set of natural scene images showed that
34 these signals provided mutually independent information (Hansen & Gegenfurtner, 2009). Jennings

1 and Martinovic (2014) described facilitatory interactions between L-M chromatic and luminance
2 signals in a task that required discriminating familiar, nameable shapes (objects) from novel,
3 unnameable shapes (non-objects). Chromatic contrast benefitted discrimination by combining with
4 co-localised luminance contrast in a facilitatory fashion, leading to reduced object/non-object
5 discrimination thresholds.

6 The brief literature overview presented above raises one important question. If chromatic
7 signals do combine with co-localised luminance signals to contribute to form perception, at which
8 stage of neural processing does this occur? With its millisecond resolution, electroencephalography
9 (EEG) is a very useful method for studying the time-course of visual processing. A specific sequence
10 of event-related potential (ERP) components are typically observed in EEG experiments that require
11 classification of visual stimuli. Some of the earlier components, such as the first positive (P1) and
12 first negative (N1) components, are more perceptual in nature, while the components that develop
13 later in the time-course reflect progressively more cognitive processing. Traditionally, these
14 components are taken as dependent variables and predictions are then made about modulations
15 that should occur due to an early, perceptual, or late, cognitive contribution. P1 and N1 components
16 are considered to be early components, reflecting perceptual processes; they are both contrast and
17 spatial-frequency dependent, and relatable to psychophysical threshold (Boon, Suttle, & Dain, 2007;
18 Souza, Gomes, Saito, da Silva, & Silveira, 2007). Isoluminant stimuli do not elicit the earliest, P1
19 component of the visual ERP but they do elicit a prominent negative deflection that corresponds in
20 timing to the N1 component (Berninger, Arden, Hogg, & Frumkes, 1989; Murray, Parry, Carden, &
21 Kulikowski, 1986). The shape of the ERP waveform is determined not only by the spatial frequency
22 and chromoluminance content of the stimulus, but also by the regularity and duration of the
23 stimulus presentation (Kulikowski, 1977; Rabin, Switkes, Crognale, Schneck, & Adams, 1994). In a
24 study that used relatively long stimulus presentations and variable intertrial intervals, typical of
25 object recognition ERP experiments, Martinovic, Mordal and Wuerger (2011) found that the
26 amplitude of the N1 component correlated with stimulus contrast. The N1 component is thus the
27 earliest locus of possible contributions of both colour and luminance to the ERP. Martinovic, Mordal
28 and Wuerger (2011) also observed object-sensitive modulations of the N1 only for images that
29 contained luminance contrast, in addition to chromatic contrast. But the N1 is not always sensitive
30 to the presence of objects (e.g., Gruber & Müller, 2005), implying that object-sensitive N1 effects are
31 likely to be reliant on stimulus and task characteristics. Object sensitivity is found much more reliably
32 in the late posterior positivity (LPP) component of the ERP, known to be robustly modulated by
33 semantic content of stimuli, e.g., their familiarity and nameability (Gruber & Müller, 2005;
34 Martinovic, Gruber, Ohla, & Muller, 2009).

1 In order to establish the way in which the time-course of object-related shape processing is
2 influenced by the presence of different contrast types in addition to luminance, we conducted an
3 ERP study. As in Jennings and Martinovic (2014), our stimuli consisted of Gaborised images of
4 objects, non-objects and pseudo-random patches. We used stimuli defined by luminance alone, as
5 well as luminance co-localised with a L-M chromatic signal and luminance co-localised with both a L-
6 M and S-(L+M) chromatic signal. Thus all of our stimuli contained luminance contrast, either on its
7 own or in combination with chromatic contrast. Comparisons between conditions that excite
8 different chromoluminant channels are complicated by the necessity to establish a common contrast
9 metric, which is far from straightforward (for a discussion, see Shevell and Kingdom, 2008). Most
10 often, contrasts in different channels are matched through multiples of threshold. We opted to set
11 our contrast levels on the basis of object/non-object discrimination thresholds from Jennings and
12 Martinovic (2014) since we intended to use the same stimulus set. Contrasts were set at threshold
13 or suprathreshold, defined as twice threshold. We intended to perform two types of analysis **on the**
14 **EEG data**. First, a traditional ERP analysis, focused on N1 and LPP components, to indicate the level
15 at which differences emerge between our object, non-object and random patch stimuli, and to
16 assess if these differences are affected by the contrast content of the stimuli. Second, linear
17 modelling of the EEG waveforms, in order to identify how three types of contrast (luminance, L-M
18 and S-(L+M)) affect the stages of processing reflected in the N1 and the LPP components. As
19 mentioned earlier, Jennings & Martinovic (2014) found that less luminance contrast was required to
20 reach threshold when it was combined with L-M chromatic contrast. Therefore, our conditions
21 significantly differed in the amount of luminance, L-M and S-(L+M) contrast they contained, enabling
22 the modelling approach.

23 We expected to find performance and early, perceptual ERP components **to be matched** at
24 threshold. At suprathreshold, we predicted that gains in performance should be matched by
25 increases in both the N1 and the LPP amplitudes. We tested whether the N1 and the LPP were
26 sensitive to differences between the three classes of stimulus images: (i) familiar, nameable shapes
27 (objects), (ii) shapes which lack familiarity and nameability (non-objects) and (iii) stimuli which lack
28 familiarity, nameability as well as any clear shape (pseudo-random patches). We expected to find
29 such sensitivity, assuming on the basis of Martinovic et al. (2011) that it was mainly driven by the
30 information derived from luminance contrast. Models that assume that luminance is more relevant
31 for object representation processes **would** predict that any object-sensitive ERP markers should be
32 more pronounced for stimuli which contain significantly more luminance. However, if this is not the
33 case, it would necessitate models of object recognition to include a shape-processing stage at which
34 chromatic contrast combines with luminance contrast (for a similar line of research with naturalistic

1 and natural images, see Groen, Ghebreab, Lamme, & Scholte, 2012; Groen, Ghebreab, Prins, Lamme,
2 & Scholte, 2013). Finally, the linear modelling of the EEG using contrast metrics would allow us to
3 directly examine the degree to which the ERP waveforms are sensitive to each type of contrast:
4 luminance, L-M or S-(L+M). In order for chromatic contrast to contribute to perceptual and cognitive
5 processing that is marked by N1 and LPP components, it needs to have a modulatory effect that is
6 circumscribed to the time-windows of these components.

9 **Materials and methods**

10 **Participants**

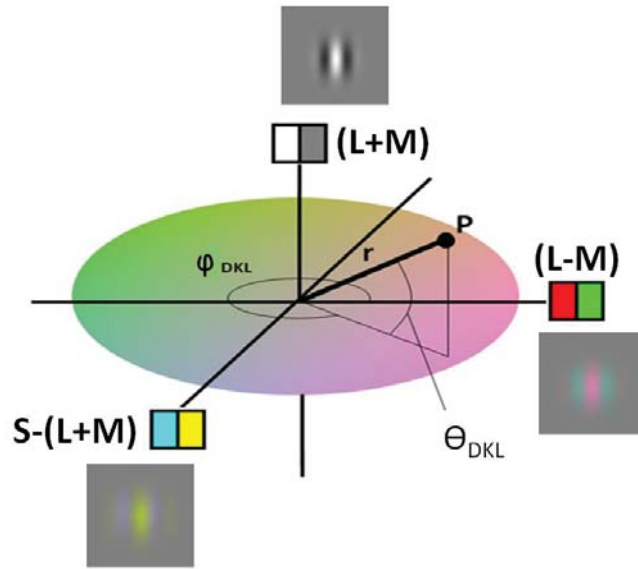
11 22 participants were recruited for the study. Each participant reported normal or corrected-to-
12 normal visual acuity and had normal colour vision as assessed with the Cambridge Colour Test (CCT;
13 Regan, Reffin, & Mollon, 1994). Three participants were excluded due to inadequate behavioural
14 performance, defined as below-chance accuracy on any single condition, and one participant was
15 rejected due to over 40% trials with artifacts. Excluded participants were replaced with new
16 participants in order to maintain counterbalancing of button-to-response allocation (see Procedure
17 section below). The final sample of 18 participants had a mean age of 25 ± 3.9 (mean \pm SD, range: 19
18 - 35 years). 16 were right-handed and 12 were female. Participants were reimbursed for their time.
19 The study was approved by the ethics committee of the School of Psychology, University of
20 Aberdeen.

21 **DKL colour space**

22 The DKL colour space (Derrington, Krauskopf, & Lennie, 1984) was used to describe the chromatic
23 properties of the stimuli. Figure 1 shows a representation of the DKL colour space indicating the two
24 chromatic (L-M and S-(L+M)) mechanisms and the luminance mechanism (L+M), along with a vector
25 (P) defining a particular chromaticity and luminance defined with a radius r , chromatic angle φ , and
26 luminance elevation Θ . The DKL space was implemented in the Colour Toolbox (CRS, UK; Westland,
27 Ripamonti, & Cheung, 2012) using measurements of monitor phosphors' spectral power
28 distributions obtained with a SpectroCAL (CRS, UK) and cone fundamentals (Stockman & Sharpe,
29 2000; Stockman, Sharpe, & Fach, 1999). A uniform mid-grey background located at the adaptation
30 point $DKL(r, \varphi, \Theta) = (0, 0, 0)$ was used throughout the experiments, this corresponded to CIE 1931 (x ,
31 y, Y) : (0.30, 0.32, 46.4), where Y has units $cd\ m^{-2}$.

32

1



2

3 **Figure 1.** The DKL colour space with three perpendicular axes corresponding to the L-M, S-(L+M) and
4 L+M mechanisms was used to specify the chromatic and luminance conditions used in this
5 experiment and further defined in Figure 2. The chromaticity and luminance at point P is described
6 by $DKL(r, \phi_{DKL}, \theta_{DKL})_{polar}$, where r is the 3-dimensional Euclidean distance from the centre of the space
7 located at $(0, 0, 0)$, ϕ_{DKL} is the chromatic angle and θ_{DKL} is the luminance elevation. The figure also
8 provides an example Gabor patch on a grey background for each of the three cardinal directions in
9 DKL space.

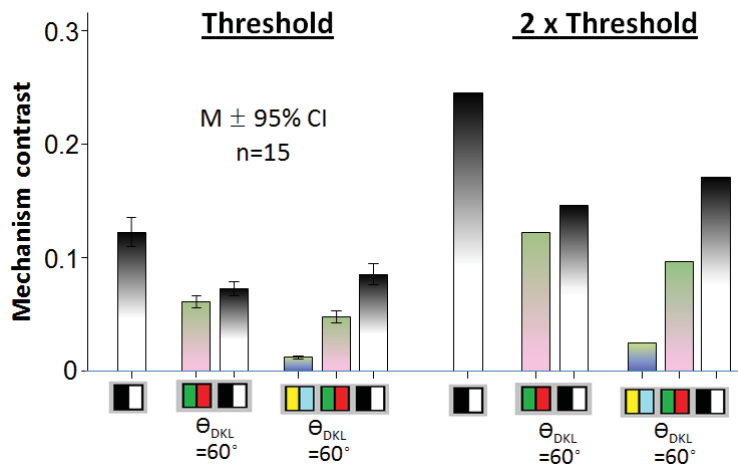
10

11 Stimulus contrast settings

12 Three different conditions were used in the study: (i) the first isolated the luminance contrast (L+M),
13 the second combined luminance and L-M contrasts, and the third combined luminance, L-M and S-
14 (L+M) contrasts. As explained in the introduction, the choice of conditions was based on object/non-
15 object discrimination results of Jennings and Martinovic (2014). We selected those combined
16 conditions in which an interaction between luminance and colour was observed, such that less
17 luminance contrast was needed in the combined condition to achieve threshold. **On the other hand,**
18 **the two conditions that combined colour and luminance did not differ significantly from each other**
19 **in terms** of L-M and L+M signals at threshold, reflecting the fact that S-(L+M) signals did not affect
20 performance. Stimuli in our study were either presented at mean object/non-object discrimination
21 threshold or at twice the threshold. This provides a range of luminance and chromatic contrasts,
22 allowing us to use linear modelling of single-trial activity by contrast in L+M, L-M and S-(L+M)
23 mechanisms.

1 Figure 2 summarises the contrasts, along with the DKL parameters. Mechanism contrasts
 2 shown in Figure 2 were derived from Michelson cone contrasts. These were calculated according to
 3 Equation 1, where I_{max} and I_{min} are the maxima and minima cone excitations of the Gabors.
 4 Mechanism contrasts were then computed for L – M, S – (L + M), and L + M.

$$C_{Michelson} = \frac{I_{max} - I_{min}}{I_{max} + I_{min}} \quad \text{Equation. 1}$$



9
 10 **Figure 2.** Contrasts for the three threshold and three suprathreshold conditions as used in the
 11 experiment. Contrasts are based on mean data of the main experiment in Jennings and Martinovic
 12 (2014).

13
 14 As mentioned earlier, it can be seen from Figure 2 that stimuli at threshold do not contain
 15 exactly the same amount of luminance contrast. If the stimuli did include the same amount of
 16 luminance, on the basis of Jennings and Martinovic's (2014) findings of facilitations between L-M
 17 and L+M signals it would be reasonable to expect improved performance for conditions combining
 18 luminance with a non-negligible amount of L-M information. This would create a problem for
 19 interpreting the results unequivocally in relation to contrast type, as differences in ERPs could also
 20 be ascribed to mismatched performance. An alternative way that would ensure matched

1 performance would have been to fix the luminance contrast at threshold and to add chromatic
2 contrast that is small enough to not affect performance. This approach would be suitable if our
3 objective was to study contrast summation without attempting to relate it to performance on a
4 shape classification task, as these chromatic contrasts would not be contributing to performance in
5 any way. Differences in contrast-response functions between luminance alone and luminance with
6 colour would warrant a separate contrast-additivity study with a much simpler stimulus and task (for
7 some previous work with EEG, see Rabin et al., 1994; Rudvin, 2005; Rudvin & Valberg, 2005). Our
8 shape discrimination task would not be suited for this purpose, as L-M and S-(L+M) isolating
9 conditions require relatively high levels of contrast at threshold (see figure 3 in Jennings and
10 Martinovic, 2014), making it impossible to stay within the CRT gamut if they were to be combined
11 with any significant levels of other contrast types.

12 | Last but not least, **in order to understand the way in which we matched stimulus contrast for**
13 **to account for performance**, it is important to note that thresholds **in Jennings and Martinovic (2014)**
14 were obtained using a two-interval forced-choice task (2IFC), in which participants had to select the
15 interval that contained the object, with the other interval containing the non-object. Therefore,
16 when we say that stimuli were presented at object/non-object discrimination threshold, this implies
17 that performance in discriminating these two categories of stimuli should be matched at this level of
18 contrast, but it does not necessarily mean that in a one-interval forced-choice (1IFC) task similar
19 accuracy rates will be obtained for object and non-object images since 1IFC tasks are additionally
20 | prone to response biases. For example, if there is **an** overall bias to classify an image as a non-object,
21 this will lead to higher error rates for objects than non-objects and higher hit rates for non-objects
22 than objects. In that case, if the hit rate for objects is 41%, with 10% of non-objects misclassified as
23 objects, the corresponding performance matches a d' of ~ 1 (thus 75% correct overall); and with the
24 hit rate for non-objects at 85% and 48% of objects misclassified as objects, the corresponding d' is
25 | again ~ 1 (matching 75% correct overall). This **shows** that discriminability **can** indeed **be** matched
26 although hit rates and error rates **for individual stimulus classes** differ. A similar approach to
27 stimulus contrast matching was successfully used in Martinovic, Mordal and Wuerger (2011) and
28 Kosilo, Wuerger, Jennings, Craddock, Hunt and Martinovic (2013). To further quantify the relations
29 between the three types of stimuli we performed an analysis of response patterns and present them
30 in Supplementary material 2. These percentages can be used to approximately assess the
31 discriminability between the different classes of stimuli, although when performing these calculations
32 it is important to account for the fact that there are three possible responses (object, non-object,
33 random). Considering that the stimuli were matched in performance using the 2IFC thresholds from
34 Jennings and Martinovic (2014), but that this does not necessarily imply that the resulting

1 performance will be 75% for each of the three stimulus classes (especially the random patches,
2 which were added as a control stimulus with no explicit contours), one could alternatively apply the
3 labels of 'lower contrast match' and 'higher contrast match' for our threshold and suprathreshold
4 conditions, respectively. We opt to use threshold and suprathreshold, as this reflects that the
5 contrasts were not chosen provisionally, but on the basis of experimental threshold data from
6 Jennings and Martinovic (2014).

7

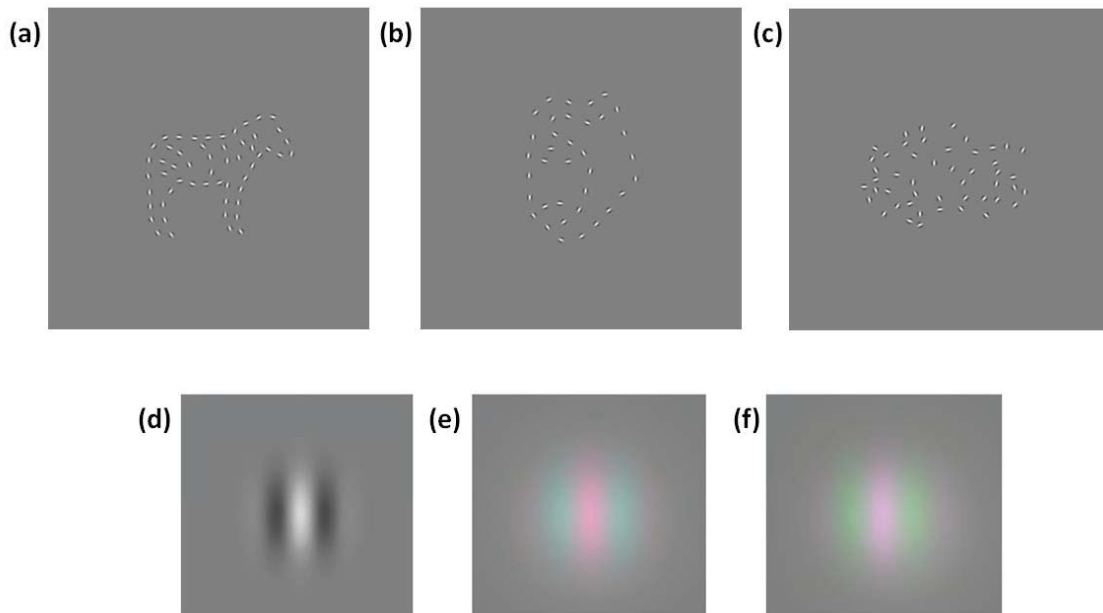
8 **Stimuli**

9 The stimulus set from Jennings and Martinovic (2014) was used (available for download at
10 <http://homepages.abdn.ac.uk/j.martinovic/pages/dept/project.htm>). This is a set of 377 Gaborised
11 nameable, familiar objects and their unnameable, unfamiliar “non-object” counterparts, similar to
12 the image library provided by Sassi and colleagues (Sassi, Machilsen, & Wagemans, 2012; Sassi,
13 Vancleef, Machilsen, Panis, & Wagemans, 2010). This stimulus set was supplemented by 377 images
14 with pseudo-randomly scattered Gabor patches, which unlike the non-objects did not consist of iso-
15 oriented contours. All stimuli were composed of a series of centre-symmetric 3 cpd Gabor patches.
16 This spatial frequency was chosen so that roughly equal contrast dependence of orientation
17 sensitivity across the mechanisms would be maintained, based on available data for L-M and
18 luminance mechanisms (Wuerger & Morgan, 1999). An additional benefit is that around 3 cpd,
19 amplitudes and latencies of S and L-M elicited VEPs are roughly similar (see Figure 9 in Rabin et al.,
20 1994). The creation of the object/non-object stimuli started by selection of suitable line images of
21 objects from various stimulus sets (Alario & Ferrand, 1999; Bates et al., 2003; Hamm & McMullen,
22 1998) and also by the manual digital drawing of additional line images of objects that were not
23 represented in those sets. The lines of these images were replaced with a series of Gabor patches
24 with the position of each Gabor patch predefined by hand in order to ensure that shape-defining
25 lines were maintained in the images (for an algorithmic approach to the same problem, see the
26 Grouping Elements Rendering Toolbox for Matlab, Demeyer & Machilsen, 2012). The corresponding
27 non-object images were created by distorting the line images of the objects until they became
28 unrecognisable using image editing software. The lines were then replaced by Gabor patches,
29 similarly to the procedure described above. Figure 3(a), (b) and (c) shows an example of an object (a
30 zebra), a non-object, and a random patch, respectively. The process of scrambling the object images
31 into non-object images attempted to preserve some important attributes of the initial object
32 images, including the visual complexity of the images as reflected in jpeg file size (Szekely and Bates,
33 2000) and their aspect ratio. In the process of transforming line-drawings into Gaborised images,

1 care was taken to have some of the lines defined by Gabor patches located near the fixation point
2 (no further than approx. 1 degree away) in order to preclude the need for eye movements to outer
3 object edges in low-contrast conditions close to threshold. Finally, the non-objects were also
4 constrained to have a closed outer contour in order be consistent with that property of objecthood
5 and preventing them from appearing as random clusters of Gabor patches, which was the added,
6 third stimulus class. These pseudo-random clusters were created by scattering the same number of
7 elements that formed the matching object and non-object pair over the approximate area that they
8 occupied as defined by an ellipse. The patches are pseudo-random as the Gabors were not allowed
9 to overlap. A pilot naming test was conducted on the stimuli, in which participants had to decide if a
10 presented shape was an object or a non-object, and then also provide a name if they classified the
11 image as an object (see Jennings and Martinovic, 2014). The final piloted set of object stimuli
12 subtended a height and width of $2.9^\circ \pm 1.0^\circ$ and $6.7^\circ \pm 1.1^\circ$ (mean \pm SD), respectively; whilst the non-
13 object stimuli subtended a height and width of $2.8^\circ \pm 0.8^\circ$ and $7.6^\circ \pm 0.9^\circ$ (mean \pm SD), respectively.
14 For more details on the Gabor properties and the attributes of the stimulus set, see Jennings and
15 Martinovic (2014).

16

17



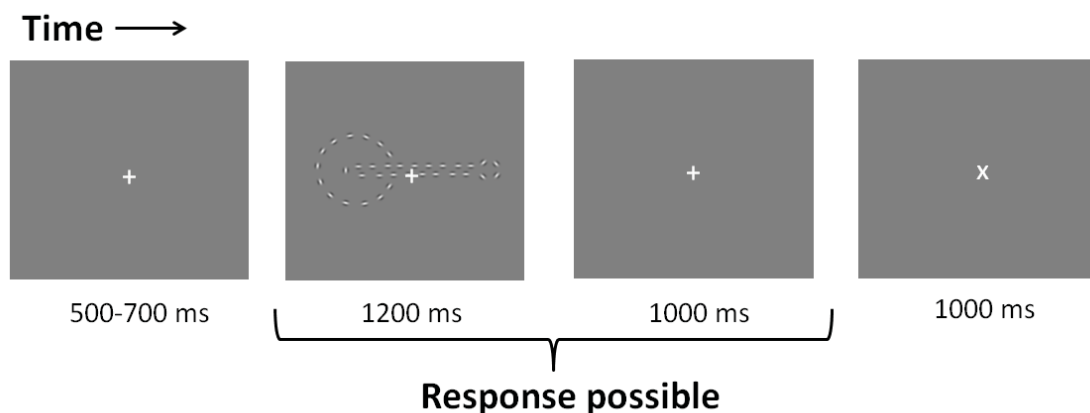
18

1 **Figure 3.** Examples of stimulus types; (a) shows an object (a zebra), (b) a non-object and (c) a
2 random patch. Examples of (d) a luminance defined, (e) a luminance and L-M modulated, and (f) a
3 luminance, L-M and S-(L+M) (i.e., the 'full' condition) modulated Gabor patches.

4 Procedure

5 Participants were informed that their task is to discriminate objects, non-objects and random
6 images. They were shown some examples of images and then performed a practice block of 51 trials
7 that contained a subset of stimuli not used in the main experiment (17 stimuli per image class). The
8 intention was to familiarize them with the task. Participants repeated the practice block if their
9 performance was below 70%. Usually, that criterion was reached after 1 repetition, sometimes no
10 repetitions were needed and rarely participants repeated the practice twice. The main experiment
11 consisted of a total of 1080 trials, distributed over ten 108-trial blocks. A trial started with a variable
12 period (500-700 ms) during which only the fixation cross was displayed, after which the stimulus was
13 displayed for 1200 ms, followed by the fixation cross only displayed for a further 1000 ms.
14 Participants responded with a button press, indicating if the presented stimulus was an object, a
15 non-object or a pseudo-random patch. Button-to-response allocation was counter-balanced across
16 participants. Participants were instructed not to make eye movements or blink during the display of
17 a stimulus or the fixation cross and to try and remain relaxed and refrain from body or head
18 movements throughout the experiment. At the end of each trial the fixation cross was replaced with
19 an "X" for 1000 ms, participants were instructed to blink during this period if required. Figure 4
20 shows the sequence of one trial.

21



22

23 **Figure 4.** Trial outlook starting with a variable period of fixation that preceded stimulus onset,
24 followed by the stimulus presentation, and ending in an additional fixation only period during which
25 observers could still respond. Finally, the fixation "+" changed to an "X" to indicate to the participant
26 that they could blink if required.

1

2 **Behavioural data analysis**

3 Accuracies and reaction times (RT) between 300 and 2200 ms were analysed. Percentage of correct
4 responses was computed for all conditions and subjected to statistical analysis, but incorrect
5 responses were also taken into consideration in an additional analysis of potential biases in response
6 patterns. Median RTs for correct items were computed for each participant. Differences in
7 accuracies and median RTs between the conditions were analysed with a repeated measures ANOVA
8 with factors *contrast level* (threshold; suprathreshold), *contrast combination* (L+M isolating; L+M
9 combined with L-M; L+M combined with both L-M and S-(L+M)), and *stimulus type* (object; non-
10 object; random patch). Greenhouse–Geiser correction was used when necessary. Post-hoc tests
11 were performed using Tukey's HSD to follow up on interactions and Bonferroni-corrected paired t-
12 tests to further assess sources of main effects. The suprathreshold data are presented in the Results
13 section, a comparison of these data with the threshold data are presented as supplementary
14 material 1. Biases in response patterns are presented as supplementary material 2.

15

16 **EEG data acquisition and analysis**

17 Continuous EEG was recorded from 128 locations using active Ag–AgCl electrodes (Biosemi
18 ActiveTwo amplifier system, Biosemi, Amsterdam, Netherlands). The typically used 'ground'
19 electrodes are replaced in the Biosemi system with two additional active electrodes. In the 128-
20 electrode montage these electrodes are positioned in close proximity to the electrode Cz and are the
21 Common Mode Sense (CMS), this acts as a recording reference and the Driven Right Leg (DRL) that
22 serves as the ground (Metting Van Rijn, Peper, & Grimbergen, 1990, 1991). Vertical and horizontal
23 electrooculograms were recorded in order to exclude trials with large eye movements and blinks.

24 EEG data processing was performed using the EEGLab toolbox (Delorme & Makeig, 2004)
25 combined with self-written procedures running under Matlab (The Mathworks, Inc, Natick,
26 Massachusetts). The EEG signal was sampled at a rate of 512 Hz and epochs lasting 2000 ms were
27 extracted, starting from 500 ms before stimulus onset and incorporating 1500 ms after stimulus
28 onset. All trials with incorrect responses were excluded from the ERP analysis. Artifact removal was
29 performed using the FASTER toolbox (Nolan, Whelan, & Reilly, 2010), followed up with a visual
30 inspection method. This left an average of 36 ± 11 (mean \pm SD) trials per condition. Further analyses
31 were performed using the average reference. A 40 Hz low-pass filter was applied to the data before
32 ERP waveform analyses. Signal-to-noise ratio (SNR) analysis was performed using the approach

1 recommended by Koenig and Melie-Garcia (2010). This was done to assess if adequate SNR was
2 reached in our experimental conditions, as ERPs at thresholds may suffer from SNR problems due to
3 the low number of trials remaining in the analysis and the relatively low amplitude of evoked
4 responses at relatively low contrast levels (Campbell & Maffei, 1970). This may in turn impact on the
5 latencies and amplitudes of ERP components. The latencies and amplitudes of the N1 component
6 and the amplitude of the LPP component at suprathreshold contrast were analysed with a repeated
7 measures ANOVA with factors *contrast combination* (L+M isolating; L+M combined with L-M; L+M
8 combined with both L-M and S-(L+M)), and *stimulus type* (object; non-object; random patch). As
9 with the behavioural data, an analysis with the additional factor of *contrast level* (threshold;
10 suprathreshold) is presented in supplementary material 1 - this analysis' main purpose was to
11 confirm that there are no differences between the three contrast combinations at threshold. The
12 components were defined based on the visual inspection of grand-mean waveforms, separately for
13 the threshold and suprathreshold components as they were expected to differ in latency (for a
14 normative study, see Porciatti & Sartucci, 1999). N1 at threshold extended from 180 ms to 380 ms,
15 while the suprathreshold N1 extended from 150 ms to 270 ms. LPP at threshold was analysed in the
16 range between 550 and 800 ms, while suprathreshold LPP was analysed between 500-750ms. In line
17 with previous literature, the N1 for a visual evoked potential with a strong chromatic component
18 was expected to occur at central occipital sites (Porciatti & Sartucci, 1999) while the LPP was
19 expected to be maximal at midline parietal sites (Gruber & Müller, 2005). Similarly to the timing of
20 components, their topographical locations were verified using grand-mean plots. Greenhouse-
21 Geiser correction was used when necessary. Post-hoc tests were performed using Tukey's HSD for
22 more complex interactions which involved 9 variables and Bonferroni-corrected paired t-tests for
23 main effects and less complex interactions which involved 6 variables. Ratios of
24 suprathreshold/threshold amplitudes were calculated using only those data points with sufficient
25 SNR. Linear modelling of the first second of the EEG single-trial data was performed using the
26 LIMO EEG toolbox for Matlab (Pernet, Chauveau, Gaspar, & Rousselet, 2011) in order to establish
27 more precisely the effect of contrast on the waveforms. For this analysis, all artifact-free trials were
28 included as per the recommendations made by VanRullen (2011), allowing us to encompass more
29 broadly how the waveforms were affected by contrast content. Linear regression analysis was
30 performed at each time-point and for each electrode based on three continuous predictors: the
31 amount of L+M, L-M and S-(L+M) contrast present in the stimulus on each trial. Following the
32 approach from Kovalenko, Chaumon and Busch (2012), we orthogonalised sequentially the three
33 parameters (Gram-Schmidt orthogonalisation method, SPM8; <http://www.fil.ion.ucl.ac.uk/spm/>).
34 The outcome of sequential orthogonalisation is that the variance that is explained by a parameter is

1 discarded from subsequent ones. This de-correlates the three types of contrast and allows us to
2 attribute effects that can be explained by more than one contrast type to just one of them.

3

4 **Results**

5 The experiment was conducted for stimuli presented at threshold and suprathreshold (i.e.,
6 $2 \times \text{threshold}$), as outlined in the Stimulus Contrast Settings section and Figure 2. It was found that
7 accuracies and ERP amplitudes measured at threshold presentation levels showed no differences
8 between the different contrast combinations employed, i.e., at threshold the stimuli were matched.
9 We hence present here only the suprathreshold data. The main differences between ERPs at
10 threshold and suprathreshold were (1) in terms of their latency, which was faster at suprathreshold,
11 and (2) in terms of the increases in amplitude with increased contrast, which were present for
12 luminance alone and L-M with luminance, but absent for the full contrast combination. Detailed
13 analyses and comparison of threshold control data and suprathreshold data (both behavioural and
14 ERPs) are presented as supplementary material 1, whilst an analysis of behavioural response biases
15 is presented as supplementary material 2.

16

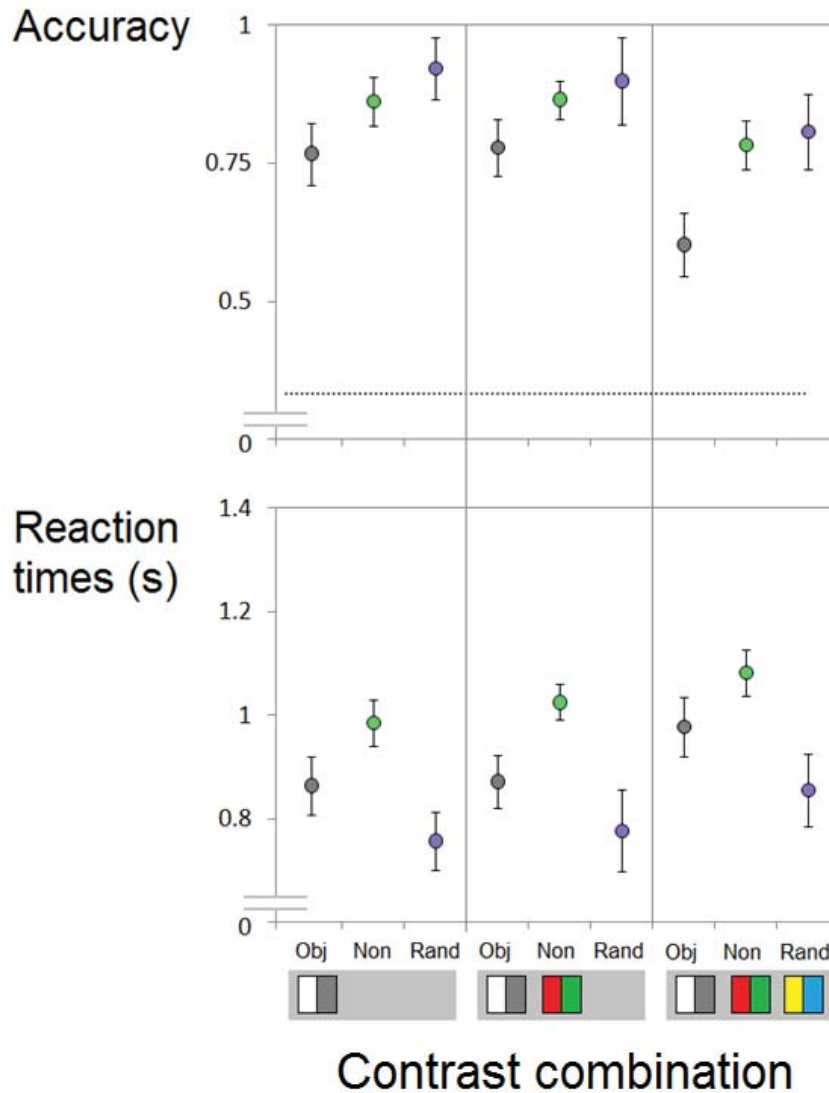
17 **Behavioural data**

18 Due to the complexity of the behavioural data analysis, covering accuracies, reaction times
19 and response patterns, we will first give an overview of the results, and then go into statistical detail.
20 Figure 5 illustrates the main findings; differences in accuracy and reaction times exist between the
21 three contrast conditions. Overall, accuracy for a given stimulus type was equal for luminance and L-
22 M with luminance conditions, and better than for the full-information contrast combination.
23 Responses were fastest for random patches, followed by objects, with non-objects eliciting the
24 slowest responses, with correct responses being lowest for object stimuli. A correlation analysis of
25 accuracy-reaction time combinations revealed no speed-accuracy trade-offs (all $p > 0.05$).

26 A 3×3 (*contrast combination by stimulus type*) repeated measures ANOVA analysis of
27 accuracies on suprathreshold data revealed significant main effects of *contrast combination* and
28 *stimulus type*; $F(2,34)=12.90$, $p < .001$, $\eta_p^2 = .43$ and $F(2,34)=41.06$, $p < .001$, $\eta_p^2 = .71$, respectively.
29 There was also a significant interaction ($F(4,68)=3.63$, $p = .01$, $\eta_p^2 = .18$).

30 Post Hoc (Tukey's HSD) tests revealed that luminance only objects were identified with the
31 same performance as L-M with luminance objects, while both were more accurately identified than

1 full-information contrast condition objects. For non-objects, there were no significant differences
 2 between the three contrast combinations. Finally, for random patch stimuli, again both had equal
 3 performance when defined with luminance only or both L-M and luminance, and both were more
 4 accurately identified than full-information contrast condition random patches. Within each contrast
 5 combination, objects were associated with poorer performance than the other two stimulus types,
 6 whilst performance between non-objects and random patches did not differ significantly.



7

8 **Figure 5.** Correct responses (top row) and corresponding reaction times (bottom row) for each
 9 chromoluminance condition at both threshold and suprathreshold. Objects: grey, Non-objects: green
 10 and random patches: purple. Error bars are 2 standard errors. Please note that the Y axis does not
 11 start at 0; the dotted grey line in the top row indicates chance level (33%).

12

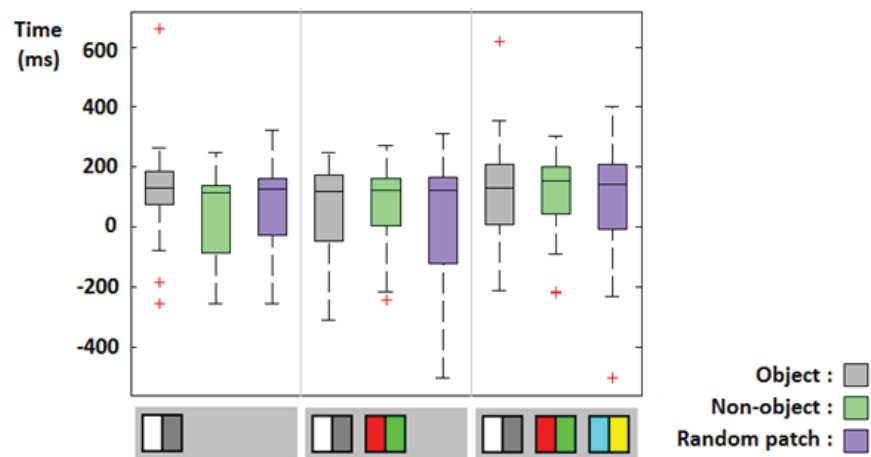
1 In terms of reaction times, there was a main effect of *contrast combination* ($F(2,34)=69.09$,
 2 $p<.001$, $\eta_p^2=.80$) and *stimulus type* ($F(2,34)=39.25$, $p=.001$, $\eta_p^2=.70$). No significant interaction
 3 existed between these levels ($F(4,68)=1.71$, $p=.092$).

4 Bonferroni-corrected t-tests informed us that performance was fastest for random patches,
 5 followed by objects, with non-objects being responded to most slowly overall (all $p_s<.001$).
 6 Performance was equally fast for luminance defined and L-M with luminance defined objects
 7 ($p=.18$), and significantly slower for the full contrast combination (both $p_s<.001$).

8 **Signal-to-noise ratios**

9 The SNRs of the ERP waveforms at suprathreshold level were assessed using the global field power
 10 permutation test recommended by Koenig and Melie-Garcia (2010). A repeated measures ANOVA
 11 revealed no significant differences in time-point of SNR stabilisation between the different stimulus
 12 types (object, non-object, random patch; $F(2,26)=1.52$, $p=.24$). Also no significant differences were
 13 found over the three luminance and colour conditions ($F(2,26)=0.62$, $p=.55$; interaction
 14 $F(4,52)=0.59$, $p=.67$). On average, an adequate SNR was reached at the following times (median \pm SE):
 15 Objects 124 ± 26 ms, non-objects 125 ± 21 ms and random patches 129 ± 28 ms, these values are
 16 collapsed over contrast combinations. For completeness the non-collapsed data is depicted in
 17 Figure 6.

18

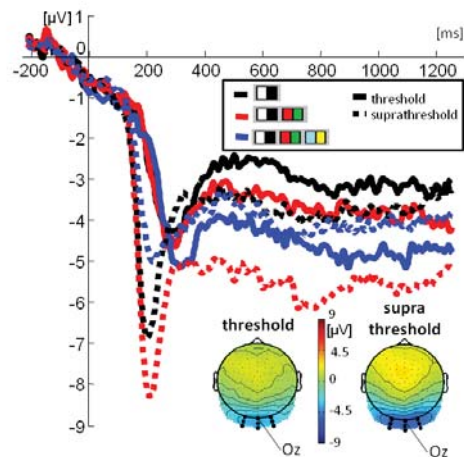


19

20 **Figure 6.** Box plots indicating the time at which the signal-to-noise ratio stabilised for all of the
 21 conditions at suprathreshold contrast levels. The stimulus types are colour coded; Objects: grey,
 22 Non-objects: green and random patches: purple. The first, second and third sub-columns represent
 23 luminance isolating, luminance combined with L-M, and Luminance combined with both L-M and S-
 24 (L+M) signals, respectively. The lines represent the median, the edges of boxes represent the 75th
 25 percentile, the ends of lines represent 95th percentile, while red crosses represent outliers.

1 Threshold and suprathreshold differences in ERP amplitudes and latencies

2 Detailed differences between threshold and suprathreshold ERPs, both in terms of their amplitudes
3 and their latencies, are presented in Supplementary Material 1. Here we give a broad overview of
4 the main contrast-related differences, which are depicted in Figure 7. This figure collapses the data
5 across different stimulus types (object, non-object, random) in order to more clearly depict changes
6 that arise due to the two-fold increase in contrast, from threshold to suprathreshold, for each
7 stimulated combination of contrasts.



8

9 **Figure 7.** Event related potential at posterior sites (see N1 topography inset), depicting data
10 collapsed across stimulus class. The full lines depict the three contrast combinations at threshold,
11 whilst the dotted lines depict them at suprathreshold. Topographies were calculated after data in the
12 N1 window (see Fig. 8) were collapsed across all conditions for threshold and suprathreshold contrast
13 levels. The electrodes which were used for data analysis are indicated on the topography plots with
14 thick black circles.

15

16 Latencies are slower for threshold stimuli, and also somewhat slower for the full
17 combination of contrasts. Ratios of suprathreshold/threshold amplitudes within the N1 analysis
18 windows were the following: luminance only, 1.64 ± 0.30 ; luminance and L-M, 1.69 ± 0.14 ;
19 luminance, L-M and S-(L+M), 1.13 ± 0.07 (M \pm SE). Ratios were only calculated from data points with
20 adequate SNR, in order to reduce the noisiness of the calculation. Whilst there is an increase in
21 amplitude for luminance alone and luminance with L-M, this does not occur for the full contrast
22 combination.

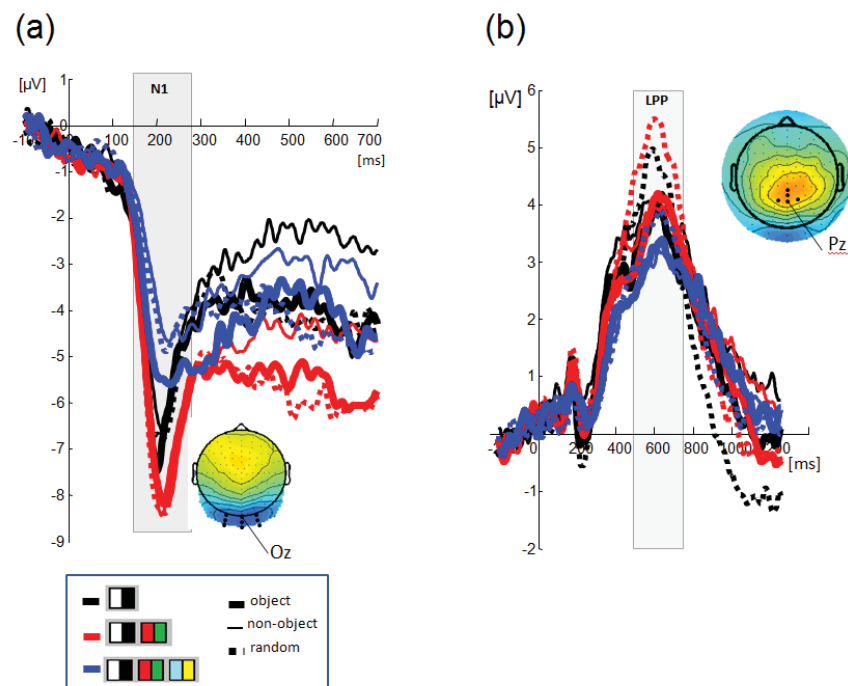
23

24

1 Event-related potentials: N1

2 The suprathreshold N1 waveform and topography are depicted in Figure 8(a), while the bar
3 plot of its amplitudes is presented in the top panel of Figure 9. There was a main effect of *contrast*
4 *combination* ($F(2,34)=30.09, p<.001, \eta p^2=.64$) and a trend towards a main effect of *stimulus type*
5 ($F(2,34)=3.11, p=.058, \eta p^2=.16$). A significant interaction existed between these levels ($F(4,68),$
6 $p=.02, \eta p^2=.15$).

7



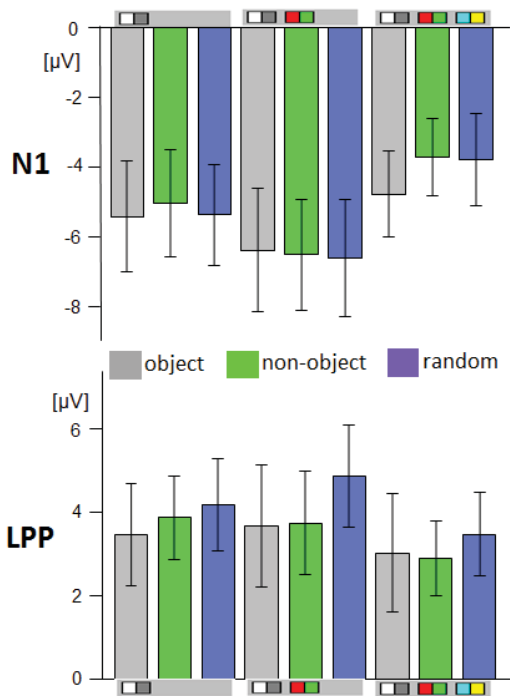
8

9 **Figure 8.** (a) N1 component of the event related potential. Waveforms at occipital sites and
10 topographies during the N1 window (indicated by the grey box) are depicted for suprathreshold
11 stimuli. (b) LPP component of the event related potential. Waveforms at parietal sites and
12 topographies during the LLP window (again indicated by the grey box) are depicted for
13 suprathreshold stimuli. In both cases, topographies were calculated after data were collapsed across
14 all conditions. The electrodes which were used for data analysis are indicated on the topography
15 plots with black circles.

16

17 Post hoc tests for the main effects indicated that the full *contrast combination* elicited the
18 least activity compared to both luminance only and L-M with luminance ($p<.05$), with luminance only
19 in turn eliciting even less activity than in the combined L-M with luminance condition ($p<.05$). Post
20 hoc tests for the interaction (Tukey's HSD) considered all possible combinations, revealing a variety

1 of differences. This was to be expected given the large main effect of *contrast combination*. But
 2 importantly, considering differences between objects, non-objects and random patches within each
 3 of the three contrast combinations, it was found that the only significant difference between
 4 stimulus types existed in the full contrast combination, here objects were found to be significantly
 5 different from non-objects and random images (both $p < .05$), which in turn did not differ amongst
 6 each other ($p > .05$).



7

8 **Figure 9.** Bar plot of ERP amplitudes. N1 is depicted in the top panel, LPP in the bottom panel. The
 9 stimulus types are colour coded - objects: grey, non-objects: green and random patches: purple. The
 10 contrast combinations are: left three bars – luminance only, middle three bars – luminance and L-M,
 11 and finally, right three bars – luminance, L-M and S-(L+M). Error bars depict +/- 2 SE.

12

13 Event-related potentials: LPP

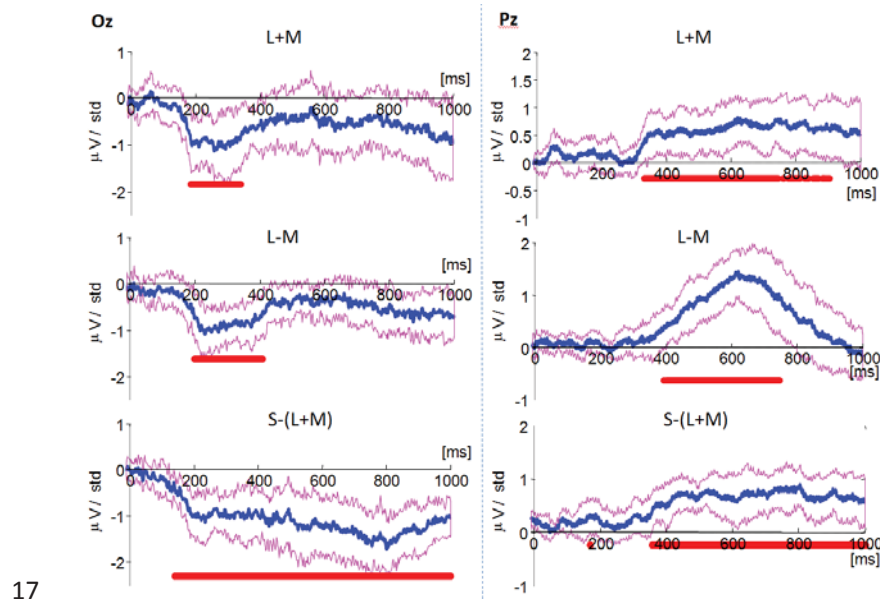
14 The late positive potential (LPP) can be seen in Figure 8(b), while the bar plot of its
 15 amplitudes is presented in the bottom panel of Figure 9. A 3x3 ANOVA (*contrast combination* by
 16 *stimulus type*) was performed and revealed main effects of both *contrast combination* and *stimulus*
 17 *type* ($F(2,34)=12.77, p < .001, \eta^2 = .43$ and $F(1.41, 23.93)=4.37, p = .036, \eta^2 = .20$, respectively. No
 18 significant interaction was discovered ($F(2.68, 45.58)=0.88, p = .45$).

19 Considering the *contrast combination* first post hoc tests revealed that the LPP had a lower
 20 amplitude for the full contrast combination as compared to both the luminance only and the

1 luminance combined with L-M combination ($p=.002$ and $p<.001$, respectively), which did not differ
2 from each other ($p=.85$). Secondly, considering *stimulus type* the LPP is higher for random patches
3 than for non-objects ($p=.015$), but there are no significant differences between objects and random
4 patches ($p=.14$) or objects and non-objects ($p=.1$).

5 **Linear modelling of single-trial EEG by contrast parameters**

6 To assess effects of each contrast type (L+M, L-M or S-(L+M)) on the ERP waveforms, we also
7 conducted a single-trial linear regression analysis using the approach described in Pernet et al.
8 (2011). We recursively orthogonalised the three contrast levels in order to de-correlate them, and
9 then entered them simultaneously into the general linear model. The results of the analysis are
10 presented in Figure 10 for electrodes Oz, exemplifying the N1 component, and Pz, exemplifying the
11 LPP component. It can be seen that all three types of contrast affect the waveforms. While the
12 effects of L+M and L-M contrasts are temporally constrained to the windows of the N1 and LPP
13 components, the effects of S-(L+M) contrast are much broader and less-specific, and although the
14 onset of contrast modulation is at approximately the same time as in the case of L+M and L-M, its
15 influence on amplitude extends in a sustained fashion throughout the analysed window and is not
16 constrained to the period of any specific component.



17

18 **Figure 10.** Linear modelling of ERP waveforms by mechanism contrasts. The left panel depicts the
19 modelling at electrode Oz, representative of the N1 component, whilst the right panel depicts the
20 modelling at electrode Pz, representative of the LPP component. The blue lines reflect the effects of
21 the model on the averaged waveform for each contrast type, with bootstrapped confidence intervals
22 shown in magenta lines. Straight red lines underneath each waveform indicate the period in which
23 the modelled effect was significant.

1 Discussion

2 This EEG study examined if the presence of chromatic contrast in luminance-defined images
3 alters both performance and neural activity during a shape classification task. Participants classified
4 Gaborised images of objects, non-objects or random patch textures defined by different
5 combinations of luminance and chromatic signals and set to mean threshold or suprathreshold
6 contrast levels. The stimuli excited either the luminance channel in isolation, or the luminance and L-
7 M channels, or the luminance and both the L-M and S-(L+M) channels simultaneously. The goal was
8 to assess the effect of chromatic contrast's **presence** through behavioural data and EEG markers of
9 perceptual and cognitive object-related processing (N1, LPP). Classification accuracy for the three
10 types of stimuli was comparable across channel combinations at threshold, confirming that the
11 contrasts were at the level that elicits matched performance. However, a mismatch appeared at
12 suprathreshold: increases in performance were less pronounced for objects defined by the full
13 combination of signals, resulting in their poorer classification. The first ERP component reliably
14 observed in the waveforms was an N1 peaking 200-300ms after stimulus onset. It occurred earlier
15 and had a larger amplitude at suprathreshold for both luminance only and luminance combined with
16 L-M conditions. The full combination at suprathreshold elicited only a shift in latency but produced
17 the same amplitude as at threshold. Some sensitivity to stimulus class was found in both N1 and LPP,
18 but it was mainly driven by different processing of random patch stimuli, **which lacked contour-**
19 **defined shape**, with LPP showing a stronger effect than the N1. Linear modelling of the EEG revealed
20 that whilst luminance and L-M contrasts modulated EEG specifically within the time-windows of the
21 perceptual and cognitive processing markers N1 and LPP, the S-(L+M) contrast had a more sustained,
22 temporally non-circumscribed effect on amplitude. The transition to suprathreshold creates
23 differences in performance for the full information stimuli, which correspond to ERP findings of less
24 amplitude gain for the full combination of contrasts. We did not find any significant differences
25 between luminance only and luminance with L-M, although the combination with L-M contained
26 much less luminance contrast. In fact, luminance and L-M contrast contributed to the amplitudes of
27 the N1 and LPP in a roughly similar fashion. Based on this, we conclude that L-M chromatic contrast
28 contributes to shape **processing** when joined with luminance contrast. Meanwhile, S-(L+M) contrast
29 does not provide a facilitatory input into these processes.

30 The waveforms we observed were characterised by an absence of a P1-like positive
31 deflection, with the first component being a relatively large N1 akin to those found in studies on
32 chromatic VEPs (Crognale, Switkes, & Adams, 1997; Murray et al., 1986; Rabin et al., 1994). The
33 absence of the P1 is likely to be due to the relatively **low level of luminance contrast in our stimuli**
34 **(for a similar finding, see Mathes & Fahle, 2007), reflected in the** late stabilisation of SNR, on average

1 between 120 and 130 ms, which is after the standard P1 window. Further, we observed differences
2 between contrast combinations when contrast level was doubled for suprathreshold stimuli. While
3 luminance alone and combined with L-M signals produces relatively uniform contrast-related N1
4 amplitude increases and performance benefits at suprathreshold, the full-channel stimulus which
5 also contained S-(L+M) information was not associated with an amplitude increase or an equivalent
6 performance benefit. Meanwhile, the latency benefit from contrast increase was uniformly present
7 across all contrast combinations, although the N1 elicited by a full combination of contrasts did lag
8 behind the other two combinations. Linear modelling demonstrated a more general effect of S-
9 (L+M) contrast on amplitude, which was not restricted to the time-window of the N1 and the LPP.
10 We did not test S-(L+M) and luminance combined nor S-(L+M) and L-M combined, so we cannot
11 conclude if the addition of S-(L+M) signals selectively suppresses the gain of the luminance
12 mechanism, of the L-M mechanism, or if it interacts with both L+M and L-M signals in this fashion.
13 An investigation of detection thresholds for S-cone increments and decrements in the presence of
14 different types of noise masks found that whilst luminance masks had a similar and weak effect on S
15 increments and decrements, chromatic masks revealed asymmetries between them by exhibiting a
16 stronger masking effect on S increments, most likely due to greater contrast gain control in the
17 unipolar S increment mechanism (Wang, Richters, & Eskew, 2014). Parametric mapping of contrast-
18 response functions for different combinations of luminance and chromatic contrasts conducted
19 across a range of spatial frequencies would extend our understanding of chromatic mechanisms
20 themselves, as well as the way in which they interact with luminance. Such experiments should also
21 attempt to model for possible contributions of chromatic aberrations to these neural signals, as
22 Forte, Blessing, Buzas and Martin (2006) have demonstrated that chromatic aberrations can produce
23 neural responses comparable in magnitude to those driven by high-frequency luminance isolating
24 stimuli.

25 Our study also aimed to assess if object-sensitivity would be found. Martinovic et al. (2011)
26 used full-information or isoluminant stimuli in an object discrimination task and concluded that
27 object-sensitivity of the N1 is brought about by the addition of an achromatic signal. However, the
28 current experiment did not find highly reliable and consistent differences between objects and non-
29 objects in the ERPs. The only object-sensitive effect in the N1 was found for the full combination of
30 contrasts. This is surprising, as luminance information is considered to be the most relevant for
31 object processing (e.g., Bar, 2003; Peterson & Gibson, 1994). The most parsimonious explanation is
32 that the full combination of signals does not scale equally with the increase in contrast for different
33 stimulus classes (see Zele, Cao, & Pokorny, 2007). If object stimuli scaled least favourably of all, this
34 would result in reduced classification performance for objects, while the larger N1 for objects could

1 perhaps be explained through increased difficulty for these stimuli. Still, it is difficult to fathom that
2 the addition of a relatively small amount of S-(L+M) contrast can have such dramatic effects on both
3 performance and on the ERP markers of visual processing, especially as the S-(L+M) signals added to
4 a mixture of L-M and L+M signals at threshold were not found to influence performance in the
5 psychophysical study of Jennings and Martinovic (2014).

6 Another difference in our findings to those of Martinovic *et al.* (2011) is that they found
7 differences in both the N1 and the LPP amplitudes elicited by line-drawings of objects as opposed to
8 non-objects, while in this study the most consistent, general effect of shape-specific processing is
9 driven by a differential response for random patches (see Fig. 8b). This is most likely to be due to
10 differences in stimulus material, and the associated difficulties of their classification. Line drawings
11 and Gaborised images are likely to engage different perceptual processes to different degrees. For
12 example, studies that compare evoked potentials elicited by greyscale photographic-quality images
13 of objects and their phase-scrambled versions find larger N1s for object images, arguing that this is
14 due to the fact that they engage figure-background processes (Schendan & Lucia, 2010). Gaborised
15 stimuli engage mid-level processes to a much higher level than line-drawings, as they require some
16 perceptual organisation in order to be correctly perceived. N1 seems to be particularly sensitive to
17 perceptual context in mid-level vision tasks (e.g., Machilsen, Novitskiy, Vancleef, & Wagemans,
18 2011). While N1 showed a series of interactions between the perceptual effects of contrast level,
19 contrast combination and stimulus type, LPP showed independent effects of these factors (for more
20 detail, see supplementary material 1). We failed to replicate previous findings of more positive late
21 potentials for non-objects than for objects, which were again obtained with line-drawing stimuli
22 (e.g., Gruber & Müller, 2005; Martinovic *et al.*, 2009; Martinovic *et al.*, 2011). However, we did find
23 increased positivity for random patches, the stimulus class that lacked contour-defined shape. It is
24 likely that the lack of differences between Gaborised objects and non-objects was due to the fact
25 that they were very closely matched. This is supported by relatively high error rates between these
26 two stimulus classes in this study (see supplementary material 2), which are much higher than in any
27 of the previous studies. The LPP was also increased for suprathreshold stimuli compared to
28 threshold stimuli, and lower for a full combination of channels, confirming its relation to successful
29 discrimination of contour-defined shapes from contour-less patches.

30 In conclusion, our study provides further evidence that signals from different channels
31 interact in the visual cortex during shape classification. L-M signals are effectively combined with
32 luminance signals at both perceptual and cognitive stages of processing, whilst S-(L+M) signals seem
33 to play a different role. Their presence results in a reduced performance benefit at suprathreshold
34 relative to other conditions, and their effects on EEG amplitude are not circumscribed to the time-

1 windows of the perceptual N1 or cognitive LPP component. These findings extend psychophysical
2 evidence that L-M contrast contributes to shape processing provided by Jennings and Martinovic
3 (2014), demonstrating that these contributions occur early in processing, in line with contrast
4 pooling studies by Groen and colleagues (2012, 2013). The model of Sowden and Schyns (2006)
5 would be able to accommodate for these findings by including signals derived from chromatic spatial
6 frequency channels (for a mathematical definition of these channels, see Zhaoping, 2014). It is
7 generally thought that S-(L+M) contrast contributes largely to colour appearance and much less to
8 spatial vision (e.g., Mollon, 1989), but we do find adverse effects on object performance and ERP
9 response amplitudes for suprathreshold stimuli that contain it. Future studies will need to establish
10 whether this is simply due to the fact that their presence alters the slopes of related psychometric
11 functions, or whether they play another, more general role in spatial vision, which would be a very
12 intriguing prospect.

13 **Acknowledgments**

14 We would like to thank Karol Puch for his assistance with data collection. This work was supported
15 by the Biotechnology and Biological Sciences Research Council (BB/H019731/1 to JM).

16

17 **References**

- 18 Alario, F. X., & Ferrand, L. (1999). A set of 400 pictures standardized for French: Norms for name
19 agreement, image agreement, familiarity, visual complexity, image variability, and age of
20 acquisition. *Behavior Research Methods, Instruments, and Computers*, *31*, 531-552.
- 21 Bar, M. (2003). A cortical mechanism for triggering top-down facilitation in visual object recognition.
22 *Journal of Cognitive Neuroscience*, *15*, 600–609.
- 23 Bates, E., D'Amico, S., Jacobsen, T., Szekely, A., Andonova, E., Devescovi, A., et al. (2003). Timed
24 picture naming in seven languages. *Psychonomic Bulletin & Review*, *10*, 344-380.
- 25 Berninger, T. A., Arden, G. B., Hogg, C. R., & Frumkes, T. (1989). Separable evoked retinal and cortical
26 potentials from each major visual pathway - preliminary results. *British Journal of*
27 *Ophthalmology*, *73*(7), 502-511.
- 28 Boon, M. Y., Suttle, C. M., & Dain, S. J. (2007). Transient VEP and psychophysical chromatic contrast
29 thresholds in children and adults. *Vision Research*, *47*(16), 2124-2133.
- 30 Campbell, F. W., & Maffei, L. (1970). Electrophysiological evidence for existence of orientation and
31 size detectors in human visual system. *Journal of Physiology-London*, *207*(3), 635-&.
- 32 Crognale, M. A., Switkes, E., & Adams, A. J. (1997). Temporal response characteristics of the
33 spatiochromatic visual evoked potential: nonlinearities and departures from psychophysics.
34 *Journal of the Optical Society of America a-Optics Image Science and Vision*, *14*(10), 2595-
35 2607.
- 36 Delorme, A., & Makeig, S. (2004). EEGLAB: an open source toolbox for analysis of single-trial EEG
37 dynamics including independent component analysis. *Journal of Neuroscience Methods*,
38 *134*(1), 9-21.

- 1 Demeyer, M., & Machilsen, B. (2012). The construction of perceptual grouping displays using GERT.
2 *Behavior Research Methods*, 44(2), 439-446.
- 3 Derrington, A. M., Krauskopf, J., & Lennie, P. (1984). Chromatic mechanisms in lateral geniculate
4 nucleus of macaque. *Journal of Physiology*, 357, 241-265.
- 5 Forte, J. D., Blessing, E. M., Buzas, P., & Martin, P. R. (2006). Contribution of chromatic aberrations to
6 color signals in the primate visual system. *Journal of Vision*, 6(2), 97-105.
- 7 Greenlee, M. W., & Magnussen, S. (1988). INTERACTIONS AMONG SPATIAL-FREQUENCY AND
8 ORIENTATION CHANNELS ADAPTED CONCURRENTLY. *Vision Research*, 28(12), 1303-1310.
- 9 Groen, I. I. A., Ghebreab, S., Lamme, V. A. F., & Scholte, H. S. (2012). Spatially Pooled Contrast
10 Responses Predict Neural and Perceptual Similarity of Naturalistic Image Categories. *PLoS*
11 *Computational Biology*, 8(10).
- 12 Groen, I. I. A., Ghebreab, S., Prins, H., Lamme, V. A. F., & Scholte, H. S. (2013). From Image Statistics
13 to Scene Gist: Evoked Neural Activity Reveals Transition from Low-Level Natural Image
14 Structure to Scene Category. *Journal of Neuroscience*, 33(48), 18814-18824.
- 15 Gruber, T., & Müller, M. M. (2005). Oscillatory brain activity dissociates between associative stimulus
16 content in a repetition priming task in the human EEG. *Cerebral Cortex*, 15, 109—116.
- 17 Hamm, J. P., & McMullen, P. A. (1998). Effects of orientation on the identification of rotated objects
18 depend on the level of identity. *Journal of Experimental Psychology: Human Perception and*
19 *Performance*, 24, 413-426.
- 20 Hansen, T., & Gegenfurtner, K. F. (2009). Independence of color and luminance edges in natural
21 scenes. *Visual Neuroscience*, 26(1), 35-49.
- 22 Jennings, B. J., & Martinovic, J. (2014). Luminance and color inputs to mid-level and high-level vision.
23 *Journal of Vision*, 14(2).
- 24 Koenig, T., & Melie-Garcia, L. (2010). A Method to Determine the Presence of Averaged Event-
25 Related Fields Using Randomization Tests. *Brain Topography*, 23(3), 233-242.
- 26 Kosilo, M., Wuerger, S. M., Craddock, M., Jennings, B. J., Hunt, A. R., & Martinovic, J. (2013). Low-
27 level and high-level modulations of fixational saccades and high frequency oscillatory brain
28 activity in a visual object classification task. *Frontiers in psychology*, 4, 948-948.
- 29 Kovalenko, L. Y., Chaumon, M., & Busch, N. A. (2012). A Pool of Pairs of Related Objects (POPORO)
30 for Investigating Visual Semantic Integration: Behavioral and Electrophysiological Validation.
31 *Brain Topography*, 25(3), 272-284.
- 32 Kulikowski, J. J. (1977). Visual evoked potentials as a measure of visibility. In J. E. Desmedt (Ed.),
33 *Visual evoked potentials in man: new developments*. Oxford: Clarendon Press.
- 34 Kulikowski, J. J. (2003). Neural basis of fundamental filters in vision. In G. T. Buracas, O. Ruksenas, G.
35 M. Boynton & T. D. Albright (Eds.), *Modulation of Neuronal Signalling: Implications for Active*
36 *Vision* (Vol. 334, pp. 3-68): NATO Science Series, Life Sciences.
- 37 Levitt, J. B., Yoshioka, T., & Lund, J. S. (1994). INTRINSIC CORTICAL CONNECTIONS IN MACAQUE
38 VISUAL AREA V2 - EVIDENCE FOR INTERACTION BETWEEN DIFFERENT FUNCTIONAL
39 STREAMS. *Journal of Comparative Neurology*, 342(4), 551-570.
- 40 Lund, J. S., Wu, Q., Hadingham, P. T., & Levitt, J. B. (1995). Cells and circuits contributing to
41 functional properties in area V1 of macaque monkey cerebral cortex: Bases for
42 neuroanatomically realistic models. *Journal of Anatomy*, 187, 563-581.
- 43 Machilsen, B., Novitskiy, N., Vancleef, K., & Wagemans, J. (2011). Context Modulates the ERP
44 Signature of Contour Integration. *PLoS ONE*, 6(9).
- 45 Martinovic, J., Gruber, T., Ohla, K., & Muller, M. M. (2009). Induced gamma-band activity elicited by
46 visual representation of unattended objects. *Journal of Cognitive Neuroscience*, 21(1), 42-57.
- 47 Martinovic, J., Mordal, J., & Wuerger, S. M. (2011). Event-related potentials reveal an early
48 advantage for luminance contours in the processing of objects. *Journal of Vision*, 11(7).
- 49 Mathes, B., & Fahle, M. (2007). The electrophysiological correlate of contour integration is similar for
50 color and luminance mechanisms. *Psychophysiology*, 44(2), 305-322.

- 1 Metting Van Rijn, A. C., Peper, A., & Grimbergen, C. A. (1990). High quality recording of bioelectric
2 events: I: interference reduction, theory and practice. *Medical and Biological Engineering*
3 *and Computing*, 28, 389-397.
- 4 Metting Van Rijn, A. C., Peper, A., & Grimbergen, C. A. (1991). High quality recording of bioelectric
5 events. II: a low noise low-power multichannel amplifier design. *Medical and Biological*
6 *Engineering and Computing*, 29, 433-440.
- 7 Mollon, J. D. (1989). THO SHE KNEELD IN THAT PLACE WHERE THEY GREW ... THE USES AND ORIGINS
8 OF PRIMATE COLOR-VISION. *Journal of Experimental Biology*, 146, 21-&.
- 9 Mullen, K. T., & Losada, M. A. (1994). Evidence for separate pathways for color and luminance
10 detection mechanisms. *Journal of the Optical Society of America*, 11, 3136-3151.
- 11 Mullen, K. T., & Losada, M. A. (1999). The spatial tuning of color and luminance peripheral vision
12 measured with notch filtered noise masking. *Vision Research*, 39(4), 721-731.
- 13 Murray, I. J., Parry, N. R. A., Carden, D., & Kulikowski, J. J. (1986). Human visual evoked-potentials to
14 chromatic and achromatic gratings. *Clinical Vision Sciences*, 1(3), 231-244.
- 15 Nolan, H., Whelan, R., & Reilly, R. B. (2010). FASTER: Fully Automated Statistical Thresholding for EEG
16 artifact Rejection. *Journal of Neuroscience Methods*, 192(1), 152-162.
- 17 Pernet, C. R., Chauveau, N., Gaspar, C., & Rousselet, G. A. (2011). LIMO EEG: A Toolbox for
18 Hierarchical Linear MOdeling of ElectroEncephaloGraphic Data. *Computational Intelligence*
19 *and Neuroscience*.
- 20 Peterson, M. A., & Gibson, B. S. (1994). Object recognition contributions to figure-ground
21 organization: Operations on outlines and subjective contours. *Perception & Psychophysics*,
22 56, 551-564.
- 23 Polat, U., & Sagi, D. (1993). LATERAL INTERACTIONS BETWEEN SPATIAL CHANNELS - SUPPRESSION
24 AND FACILITATION REVEALED BY LATERAL MASKING EXPERIMENTS. *Vision Research*, 33(7),
25 993-999.
- 26 Porciatti, V., & Sartucci, F. (1999). Normative data for onset VEPs to red-green and blue-yellow
27 chromatic contrast. *Clinical Neurophysiology*, 110(4), 772-781.
- 28 Rabin, J., Switkes, E., Crognale, M., Schneck, M. E., & Adams, A. J. (1994). Visual-evoked potentials in
29 3-dimensional color space - correlates of spatiochromatic processing. *Vision Research*,
30 34(20), 2657-2671.
- 31 Regan, B. C., Reffin, J. P., & Mollon, J. D. (1994). Luminance noise and the rapid determination of
32 discrimination ellipses in color deficiency *Vision Research*, 34(10), 1279-1299.
- 33 Rudvin, I. (2005). Visual evoked potentials for reversals of red-green gratings with different
34 chromatic contrasts: Asymmetries with respect to isoluminance. *Visual Neuroscience*, 22(6),
35 749-758.
- 36 Rudvin, I., & Valberg, A. (2005). Visual evoked potentials for red-green gratings reversing at different
37 temporal frequencies: Asymmetries with respect to isoluminance. *Visual Neuroscience*,
38 22(6), 735-747.
- 39 Sassi, M., Machilsen, B., & Wagemans, J. (2012). Shape detection of Gaborized outline versions of
40 everyday objects. *i-Perception*, 3(10), 745-764.
- 41 Sassi, M., Vancleef, K., Machilsen, B., Panis, S., & Wagemans, J. (2010). Identification of everyday
42 objects on the basis of Gaborized outline versions. *i-Perception*, 1(3), 121-142.
- 43 Schendan, H. E., & Lucia, L. C. (2010). Object-sensitive activity reflects earlier perceptual and later
44 cognitive processing of visual objects between 95 and 500 ms. *Brain Research*, 1329, 124-
45 141.
- 46 Shevell, S. K., & Kingdom, F. A. A. (2008). Color in complex scenes. *Annual Review of Psychology*, 59,
47 143-166.
- 48 Solomon, S. G., & Lennie, P. (2007). The machinery of colour vision. *Nature Reviews Neuroscience*,
49 8(4), 276-286.
- 50 Souza, G. S., Gomes, B. D., Saito, C. A., da Silva, M., & Silveira, L. C. L. (2007). Spatial luminance
51 contrast sensitivity measured with transient VEP: Comparison with psychophysics and

1 evidence of multiple mechanisms. *Investigative Ophthalmology & Visual Science*, 48(7),
2 3396-3404.

3 Sowden, P. T., & Schyns, P. G. (2006). Channel surfing in the visual brain. *Trends in Cognitive*
4 *Sciences*, 10(12), 538-545.

5 Stockman, A., & Sharpe, L. T. (2000). Spectral sensitivities of the middle- and long-wavelength
6 sensitive cones derived from measurements in observers of known genotype. *Vision*
7 *Research*, 40, 1711-1737.

8 Stockman, A., Sharpe, L. T., & Fach, C. (1999). The spectral sensitivity of the human short-wavelength
9 sensitive cones derived from thresholds and color matches. *Vision Research*, 39(17), 2901-
10 2927.

11 Tanaka, J. W., Weiskopf, D., & Williams, P. (2001). The role of color in high level vision. *Trends in*
12 *Cognitive Sciences*, 5, 211-215.

13 Tolhurst, D. J. (1972). ADAPTATION TO SQUARE-WAVE GRATINGS - INHIBITION BETWEEN SPATIAL
14 FREQUENCY CHANNELS IN HUMAN VISUAL SYSTEM. *Journal of Physiology-London*, 226(1),
15 231-&.

16 VanRullen, R. (2011). Four common conceptual fallacies in mapping the time course of recognition.
17 *Frontiers in psychology*, 2.

18 Vidyasagar, T. R., Kulikowski, J. J., Lipnicki, D. M., & Dreher, B. (2002). Convergence of parvocellular
19 and magnocellular information channels in the primary visual cortex of the macaque.
20 *European Journal of Neuroscience*, 16(5), 945-956.

21 Wang, Q. H., Richters, D. P., & Eskew, R. T. (2014). Noise masking of S-cone increments and
22 decrements. *Journal of Vision*, 14(13).

23 Webster, M. A., DeValois, K. K., & Switkes, E. (1990). Orientation and spatial-frequency
24 discrimination for luminance and chromatic gratings. *Journal of the Optical Society of*
25 *America*, 7(6), 1034-1049.

26 Westland, S., Ripamonti, C., & Cheung, V. (2012). *Computational Colour Science Using MATLAB 2nd*
27 *Edition*: John Wiley & Sons.

28 Wuerger, S. M., & Morgan, M. J. (1999). The input of the long- and medium wavelength sensitive
29 cones to orientation discrimination. *Journal of the Optical Society of America*, 16(3), 436-
30 442.

31 Wuerger, S. M., Morgan, M. J., Westland, S., & Owens, H. (2000). The spatio-chromatic sensitivity of
32 the human visual system. *New Journal of Physics: Physiological Measurements*, 21(11), 505-
33 513.

34 Zele, A. J., Cao, D. C., & Pokorny, J. (2007). Threshold units: A correct metric for reaction time? *Vision*
35 *Research*, 47(5), 608-611.

36 Zhaoping, L. (2014). *Understanding Vision: Theory, Models, and Data*. Oxford: Oxford University
37 Press.

38

39